



Bystander Response Following High-Dose X-irradiation; Time-dependent Nature of GammaH2AX Foci and Cell Death Consequences

Fatemeh Pakniyat (PhD)¹, Hossein Mozdarani (PhD)^{2*}, Hassan Ali Nedaie (PhD)^{1,3}, Aziz Mahmoudzadeh (PhD)⁴, Mahdieh Salimi (PhD)⁵, Somayeh Gholami (PhD)³

ABSTRACT

Background: The paradigm shifts in target theory could be defined as the radiation-triggered bystander response in which the radiation deleterious effects occurred in the adjacent cells.

Objective: This study aims to assess bystander response in terms of DNA damage and their possible cell death consequences following high-dose radiotherapy. Temporal characteristics of gH2AX foci as a manifestation of DNA damage were also evaluated.

Material and Methods: In this experimental study, bystander response was investigated in human carcinoma cells of HeLa and HN5, neighboring those that received high doses. Medium transfer was performed from 10 Gy-irradiated donors to 1.5 Gy-irradiated recipients. GammaH2AX foci, clonogenic and apoptosis assays were investigated. The gH2AX foci time-point study was implemented 1, 4, and 24 h after the medium exchange.

Results: DNA damage was enhanced in HeLa and HN5 bystander cells with the ratio of 1.27 and 1.72, respectively, which terminated in more than two-fold clonogenic survival decrease, along with gradual apoptosis increase. GammH2AX foci temporal characterization revealed maximum foci scoring at the 1 h time-point in HeLa, and also 4 h in HN5, which remained even 24 h after the medium sharing in higher level than the control group.

Conclusion: The time-dependent nature of bystander-induced gH2AX foci as a DNA damage surrogate marker was highlighted with the persistent foci at 24 h. considering an outcome of bystander-induced DNA damage, predominant role of clonogenic cell death was also elicited compared to apoptosis. Moreover, the role of high-dose bystander response observed in the current work clarified bystander potential implications in radiotherapy.

Citation: Pakniyat F, Mozdarani H, Nedaie HA, Mahmoudzadeh A, Salimi M, Gholami S. Bystander Response Following High-Dose X-irradiation; Time-dependent Nature of GammaH2AX Foci and Cell Death Consequences. *J Biomed Phys Eng.* 2023;13(1):17-28. doi: 10.31661/jbpe.v0i0.2001-1053.

Keywords

Bystander; High-Dose; GammaH2AX; DNA Damage; Survival; Apoptosis

Introduction

Accumulating evidence of non-targeted effect (NTE) has been challenged as the classical dogma in radiation biology which demonstrated the radiation adverse effects in only directly-irradiated cell populations. One of these paradigm shifts in target response was defined as the radiation-induced bystander effect (RIBE) in which

¹Department of Medical Physics and Biomedical Engineering, Tehran University of Medical Sciences, Tehran, Iran

²Department of Medical Genetics, Faculty of Medical Sciences, Tarbiat Modares University, Tehran, Iran

³Radiation Oncology Research Center, Cancer Institute, Tehran University of Medical Sciences, Tehran, Iran

⁴Department of Bioscience and Biotechnology, Malek-Ashtar University of Technology, Tehran, Iran

⁵Department of Medical Genetics, Medical Biotechnology Institute, National Institute of Genetic Engineering and Biotechnology, Tehran, Iran

*Corresponding author: Hossein Mozdarani
Department of Medical Genetics, Faculty of Medical Sciences, Tarbiat Modares University, Tehran, Iran
E-mail: mozdarah@modares.ac.ir

Received: 19 January 2020
Accepted: 7 May 2020

radiation effect was occurred in the adjacent cells. This off-target concept was pioneered by Nagasawa and Little who observed RIBE in low-dose range of α particle at first [1]. Soon afterwards, the bulk of studies were conducted, examining the RIBE under the *in vitro* and *in vivo* distinct experimental circumstances [2, 3] along with different radiation doses and quality properties [4-6]. Moreover, the definition of bystander cells has included different categories from zero-irradiated neighboring cells to the irradiated neighboring cells [7]. The exact mechanism underlying the RIBE was not completely understood and distinct signaling pathways might be stimulated. However, *in vitro* evaluation was consisted of two different approaches, including medium transfer and cell-to-cell contact. Medium transfer RIBE was recognized as the bystander signal transduction using diffusible factors transferred from directly-irradiated cells to non-target ones, not requiring cells physical contact [8]. The cell-to-cell contact RIBE was involved by gap junction intracellular communication (GJIC), requiring cells physical contact [9].

Up to now, RIBE has been evaluated by the use of various biomarkers, including DNA damage, cell death, gene expression modifications, and chromosomal aberrations. DNA double-strand breaks (DSBs) have been introduced as another endpoint, manifesting the RIBE. Amongst ionizing radiation-induced DNA damage, DSBs are generally considered as the most lethal damage due to its error-prone repair mechanism which might bear a high risk for the genome stability, leading to lethal consequences [10]. Some evidence targeted the DSBs function in RIBE [11-16] and it has been well documented that Ser139 rapid phosphorylation on the specialized histone H2AX formed the gH2AX as an early response to DSBs induction. gH2AX assay using specific fluorescent antibodies, expressed as discrete nuclear foci, was considered to monitor DSBs [17]. Distinct reports of RIBE have been elicited using gH2AX foci assay, expressing

DSBs enhanced numbers in bystander cells [13, 18, 19]. From the standpoint of bystander gH2AX foci formation, time-point study was regarded as priority and earlier researches have been accumulating in order to investigate this trend particularly in low-dose levels as a result reporting different conclusions [18-23].

RIBE has been formerly confirmed as a more pronounced phenomenon at low dose, illustrating the saturation in high-dose level or proposing an on-off mannerism [24]. Alternatively, evidence corroborated the bystander occurrence in high-dose levels particularly in the radiation therapy [25, 26]. However, radiation-triggered bystander cell death in radiation therapy was regarded as an ambiguous issue [27]. Bystander response may encompass a number of obvious merits in radiotherapy especially using the non-uniform irradiation strategy, including Grid treatment. Grid hypofraction technique to treat the bulky advanced tumors could create the inhomogeneous dose distribution by several pencil beam fields using perforated lead or cerrobend block and multileaf collimator [28].

As many reports of RIBE manifestations were in agreement with the DNA damage, time-dependency nature of bystander-induced DSBs in high-dose area could be very important. Therefore, the primary purpose of this study was to evaluate the medium transfer RIBE in high-dose levels, which was consistent with Grid hypofractionation technique. More importantly, bystander-triggered gH2AX foci temporal characteristic along with final cell death results were investigated in two distinct tumor cell lines.

Material and Methods

Cell culture

In this experimental study, two different cell lines of human head and neck squamous cell carcinoma (HN5) and human cervix carcinoma (HeLa) were provided from the National Cell Bank of the Pasteur Institute (Tehran,

Iran). HN5 and HeLa were cultured as monolayers in RPMI1640 and DMEM (Dulbecco's Modified Eagle's) mediums, respectively, supplemented with 10% Fetal Calf Serum (FCS) (Gibco-BRL), antibiotics (Penicillin 100 iu/ml and Streptomycin 100 μ g/ml) (Gibco-BRL), remaining at 37 °C in a humidified 5% CO₂ incubator.

Irradiation setup

Since the bystander response evaluation after clinical Grid treatment was carried out, consequently, it was crucial to expose the cells uniformly by the dose obtained from the peak-to-valley dose curve of the Grid block available in the Cancer Institute (Figure 1) [29]. According to the dosimetry validation, when the single fraction of 10 Gy was applied, the Grid aperture center (peak region) received 10 Gy at Dmax; while the Grid block center (valley region) received an average dose of 1.5 Gy. Water-equivalent slabs with total thickness of 2 cm at the top and 6 cm under the cell dishes were placed to achieve source to skin distance (SSD) of 100 cm. Following Grid irradiation, the RIBE could be occurred within the irradiated tumor cells and the bystander cells were located under shielded (lower dose) regions of the Grid. Therefore, using the medium transfer strategy of bystander evaluation, donor and recipient cells were exposed uniformly by 10 Gy and 1.5 Gy, respectively using Varian 2100 C linear accelerator (Linac) of 6 MV photon beam, with the 20 cm \times 20 cm field size at the isocenter.

Medium Transfer Bystander study

Exponentially growing cells were seeded in T-25 culture flasks, which were consisted of 5 ml culture medium 48 h before the treatment in triplicate. After donor and recipient cells irradiation, specific incubation time of 1 and 4 h was applied in order to achieve the maximum bystander signal. The medium of recipients (bystander cells) was removed and replaced by the conditioned medium, which was the

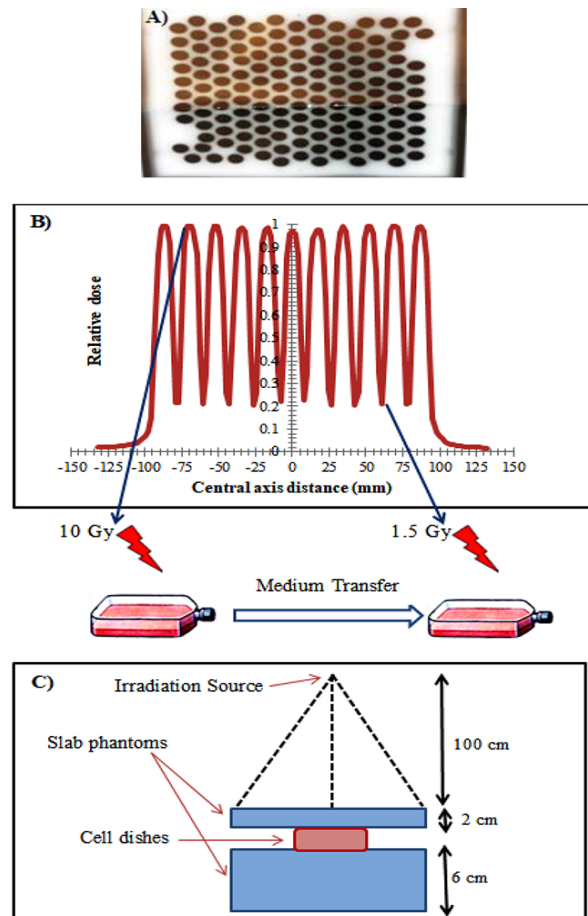


Figure 1: A) The image of Grid pattern which was consisted of circular fields; B) The Grid in-plane dose profile measured by ionization chamber: medium transfer irradiation was performed based on the peak-to-valley dose profile curve; and C) Schematic view of irradiation setup.

donors filtered medium (target cells) by the means of 0.22 μ m filter, eliminating all cells and all cellular debris, except those soluble factors from the medium.

Colony Formation Assay

Medium exchange was implemented 4 h after the irradiation, and after 24 h-incubation at the temperature of 37 °C, the colony formation assay as a radiobiological "gold standard" technique was performed. Cells were seeded in sparsely definite numbers. By passing the 10 to 14 days from the incubation time, the colonies

(>50 cells) were formed and stained by 0.5% of crystal violet (Sigma- Aldrich, USA), and then counted under a light microscope (Nikon, YS100, Japan). Plating efficiency (%PE) was ascertained as the ratio of the number of counted colonies to the seeded cells. Also, survival fraction (%SF) was achieved by normalizing efficiencies of the irradiated groups to the control group. Survival fraction at 2 Gy (SF2) was calculated to compare the radiosensitivity.

GammaH2AX Immunofluorescence Assay

DSBs of directly-irradiated and bystander cells were assessed using immunofluorescence detection of phosphorylated H2AX histones. Moreover, definite time points were assigned in order to evaluate the gH2AX foci kinetics. Specific incubation time of 1 and 4 h were used post irradiation, and after that cell harvesting and gH2AX assay were initiated by passing 1 h, 4 h, and 24 h from the medium transfer. Briefly explained, 2×10^5 cells were seeded into slides and fixed in 4% formaldehyde followed by PBS washing. Premeabilization was performed by the use of 0.25% Triton-X-100, and was blocked with 1% bovine serum albumin (BSA) accompanying with 0.05% Tween. Afterwards, 2-hour primary antibody incubation with 100 μ lit of anti-phospho-histone H2AX antibody (Millipore) was performed under the wet-chamber setting followed by BSA washing. Also, 45-min secondary antibody incubation was performed with 100 μ lit of anti-mouse IgG-FITC (Sigma-Aldrich, USA) antibody in dim lighted wet-chamber followed by PBS washing. FPC scoring was exerted after Dapi (Abnova, Taiwan) staining by the use of OLYMPUS fluorescence microscope equipped with U/B/G, FITC, TXRED, DAPI filters in a meticulous consideration by eyes.

Annexin V-FITC apoptosis Staining Assay

By passing 4 h from the irradiation, medium transfer was implemented and Annexin

staining assay was conducted at the specific time of 24 h as an apoptosis induction appropriate interval [30]. Annexin apoptotic assay was initiated by the use of FITC Annexin V Staining Kit (BioLegend), in accordance with the manufacturer's instruction. Briefly, 5×10^5 cells were resuspended in 200 microliters of binding buffer (1 \times), and five microliters of Annexin V- FITC was added to each sample then incubated for 15 min at room temperature in the dark, followed by addition of 10 microliters of PI (20 μ g/ml) as well. Samples were analyzed for the apoptotic and necrotic cells presence by the use of BD FACS Calibur flow cytometer (BD Bioscience). 10,000 calls per each sample were evaluated and the obtained data were analyzed using the BD Cell Quest Pro software.

Statistical Analysis

The studied groups comprised 0 Gy control, 1.5 Gy medium transfer bystander, and 1.5 Gy open field. To compare whether the enhancement level, resulting from probable bystander response, was more or less than the damage caused by typical dose of 2 Gy as a routine conventional fractionation, a 2 Gy open field was also evaluated. Statistical analysis was performed using SPSS software (version 24). All data were expressed in terms of the mean values \pm standard error of the mean (SEM) for each group, and also were analyzed by the One-Way ANOVA test. P value less than 0.05 was considered as a significant level.

Results

Colony Formation Assay

Survival fraction at 2 Gy (SF2) of HeLa and HN5 was determined as 0.42 ± 0.06 and 0.5 ± 0.03 , respectively, proposing more radioresistance of HN5. The acquired results indicated RIBE as defined by the statistically significant clonogenic formation decrease ($P < 0.05$) in 1.5 Gy bystander groups in comparison with those cells merely exposed by 1.5

Gy (Figure 2). The plating efficiency (PE) of 1.5 Gy open field decreased approximately by two times in HeLa medium transfer bystander. However, this descending rate approximately by three times was more remarkable in HN5. Table 1 indicated the SF results.

Gamma H2AX Assay

Gamma H2AX foci per cell (FPC) was scored qualitatively, and also processed using Image J software 1.50i (Figure 3). In total, the FPC ascending trend was obvious from directly-irradiation of 1.5 Gy to the bystander groups in both cell lines, implying the increasing number of DNA DSBs in the adjacent cells

Table 1: Survival Fraction (%SF) of HeLa and HN5 groups.

Groups	SF%±SEM	
	HeLa	HN5
1.5 Gy Open-field	62.98±1.95	70±1.58
1.5 Gy Bystander	*32.88±1.52	*24.02±0.31
2 Gy Open-field	42.35±6.15	50.27±3.22

SF: Survival Fraction

Data expressed as mean±standard error of the mean (SEM) of three independent experiments; * indicated the statistically significant difference between 1.5 Gy open field and bystander groups.

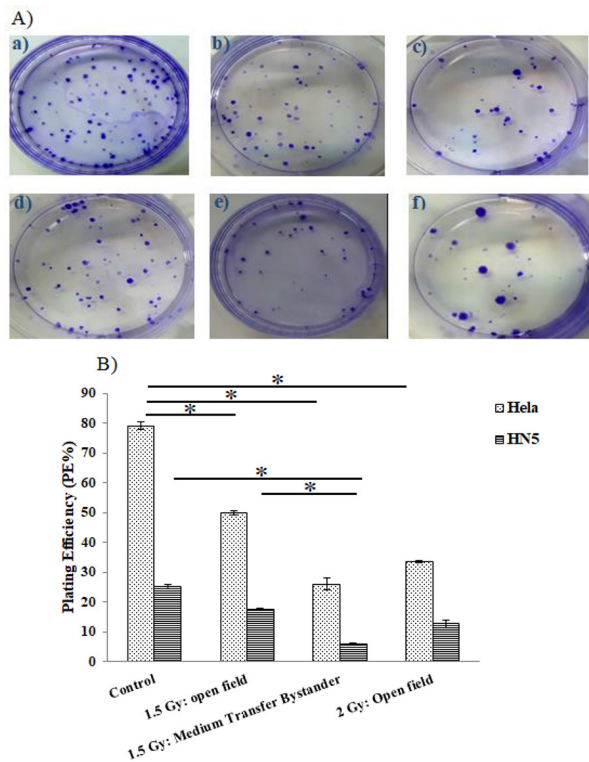


Figure 2: A) Clonogenic formation figures stained with crystal violet; a) Control of HeLa; b) HeLa 1.5 Gy open-field; c) HeLa 1.5 Gy bystander; d) Control of HN5; e) HN5 1.5 Gy open-field; and f) HN5 1.5 Gy bystander. B) Plating efficiencies (%PE) in HeLa and HN5 different samples. *P<0.05.

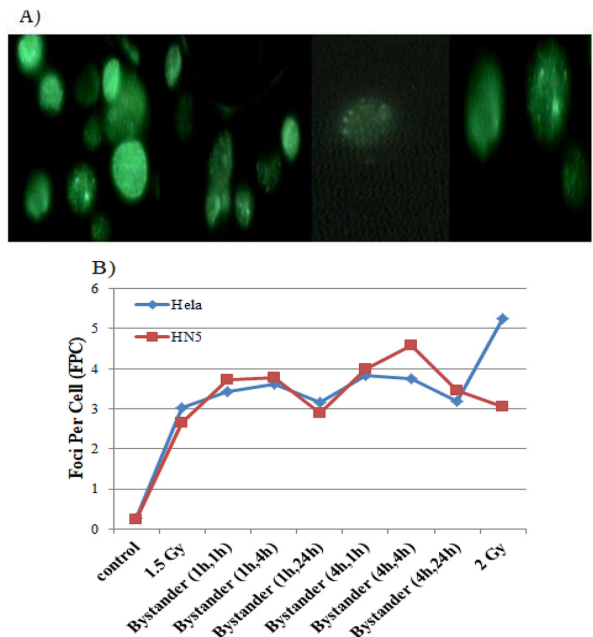


Figure 3: GammaH2AX foci scored using fluorescence microscope under fluorescein isothiocyanate (FITC) filter. A) Cells with distinct foci per cell (FPC); B) Time-point groups of bystander-induced gH2AX foci included different incubation time before/ after medium transfer (1 h or 4 h / 1 h, 4 h, and 24 h): Illustrated by the trend of FPC observed in HeLa and HN5 groups, the DNA double strand breaks (DSBs) in HeLa bystander cells were less and in HN5 more than the levels induced by 2 Gy. *P<0.05.

and more significant in HN5. The FPC of HeLa bystander groups verified the peak of 4 h/ 1 h (3.83 ± 0.23), and also trough of 1 h/ 24 h (incubation time before/ after medium transfer), in comparison with the 4 h/ 4 h (4.59 ± 0.07) and 1 h/ 24 h in HN5, respectively (Table 2). Along with the upward trend in bystander cells, DNA DSBs in HeLa were less and in HN5 were more than those induced by 2 Gy. It is noteworthy to state that between the FPC maximum and minimum values, no statistically significant difference was observed in the HeLa bystander groups, while the statistically significant distinction was considered in HN5. The “gH2AX enhancement ratio” of HeLa and HN5 defined as the FPC of bystander cells to the value obtained from 1.5 Gy directly-irradiation was 1.27 and 1.72, respectively.

Annexin Staining Assay

The apoptotic findings demonstrated the

Table 2: Foci per cell (FPC) scored in different groups of HeLa and HN5.

Groups	Mean of FPC±SEM	
	HeLa	HN5
Control	0.273±0.005	0.227±0.003
1.5 Gy Open-field	3.027±0.612	2.660±0.191
1.5 Gy Bystander (1 h, 1 h)	3.423±0.127	3.727±0.190
1.5 Gy Bystander (1 h, 4 h)	3.630±0.806	3.780±0.735
1.5 Gy Bystander (1 h, 24 h)	3.160±0.848	2.889±0.080
1.5 Gy Bystander (4 h, 1 h)	3.833±0.237	4.003±0.109
1.5 Gy Bystander (4 h, 4 h)	3.755±1.025	4.590±0.071
1.5 Gy Bystander (4 h, 24 h)	3.193±0.196	3.470±0.156
2 Gy Open-field	5.255±0.078	3.045±0.064

FPC: Foci per cell

Data expressed as mean±standard error of the mean (SEM) of three independent experiments

gradual apoptotic increase in the adjacent cells that experienced medium exchange (Figure 4). However, this difference was not statistically significant. The “apoptotic enhancement ratio” of HeLa and HN5 defined as the bystander cells apoptotic percentage to the value of 1.5 Gy directly-irradiation was 1.77 and 1.11, respectively. Noteworthy, all necrosis values were almost less than 3% and consequently, considered as negligible.

Discussion

This research assessed the high-dose RIBE consistent with the Grid hypo-fractionation technique in two distinct tumor cell lines with central focus on the bystander-induced gH2AX foci temporal trait, and its relationship with cell death. Medium transfer evaluation was exerted in order to investigate that the transmissible factor from the high-dose irradiated cells could result in the deleterious effect on the adjacent ones. RIBE as a stress response could be defined by the use of gH2AX endpoint with foci elevated number along with other DNA damage response (DDR) indicating DNA DSBs induction [31]. Broad range of studies on RIBE of α interaction indicated the greater fraction of positive cells with DSBs in comparison with those that actually traversed α -particles, and also indicated the gH2AX foci co-localization and other DDR factors involvement [18, 19]. Moreover, low-LET irradiation investigation by Yang et al. indicated more gH2AX foci in bystander cultures in comparison with the control group in a dose-independent trend [13]. Parallel with these reports, our research results focusing on X-ray high-dose irradiation revealed higher frequency of FPC (foci per cell) in bystander cells receiving 1.5 Gy in comparison with 1.5 Gy direct-irradiation, which might imply the RIBE occurrence.

As a main focus, this research outlined the temporal characteristic of gH2AX foci as an early and sensitive biomarker of DNA DSBs. A great wealth of evidence revealed the grow-

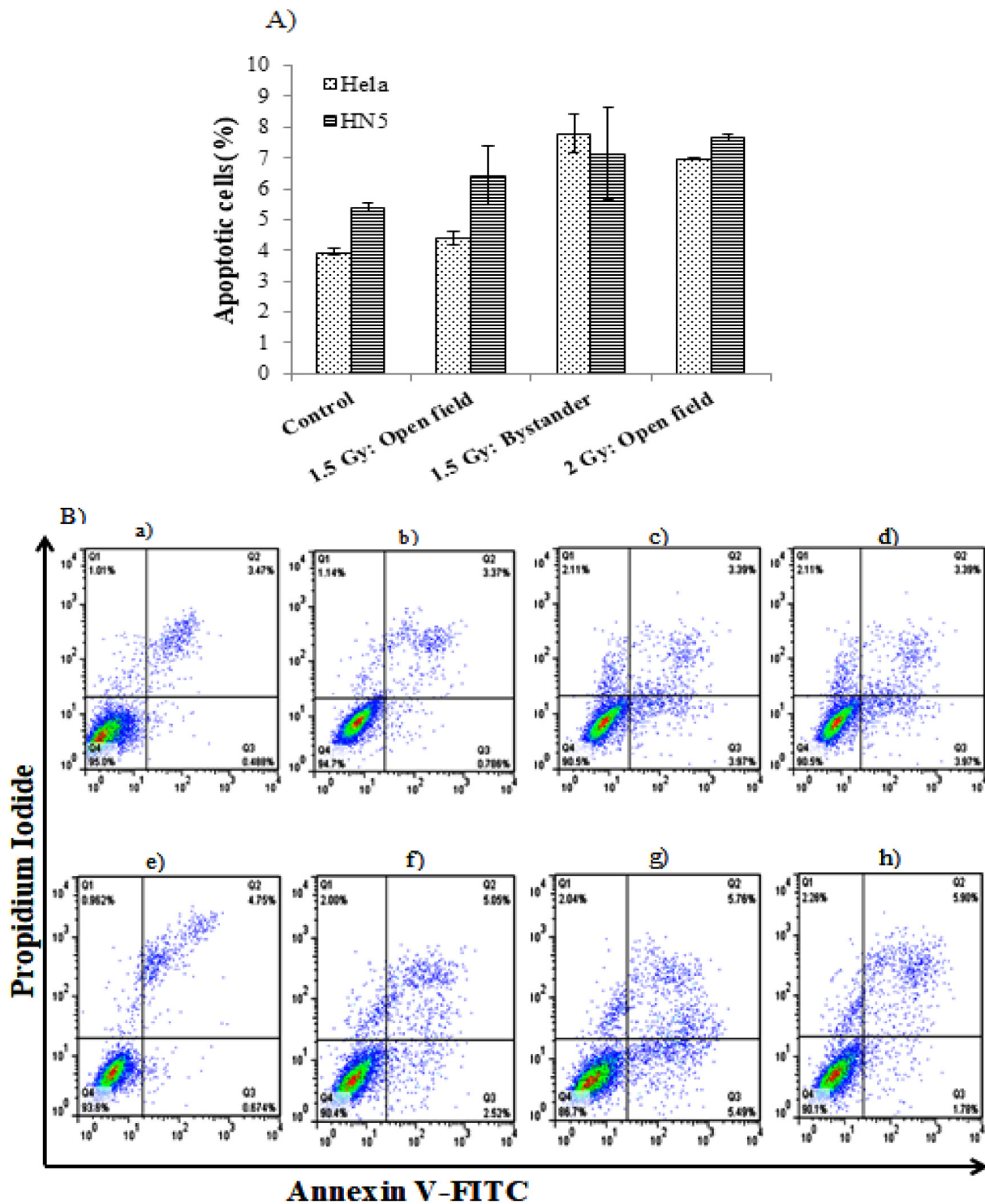


Figure 4: A) Flowcytometry of apoptosis induction in cell lines of HeLa and HN5 based on Annexin V-FITC (fluorescein isothiocyanate) and Propidium Iodide (PI) double staining and B) Scatter plots of apoptosis in a) HeLa untreated control; b) HeLa 1.5 Gy open field; c) HeLa 1.5 Gy bystander; d) HeLa 2 Gy open-field; e) HN5 untreated control; f) HN5 1.5 Gy open-field; g) HN5 1.5 Gy bystander; and h) HN5 2 Gy open-field. (Data expressed as mean \pm standard error of the mean (SEM) of three independent experiments).

ing consensus about the gH2AX foci time-dependent nature particularly in low-dose level, but fundamental questions could be responded and at the top of this agenda might be the initiation and peak time of bystander signaling considering the high dose. Our observations of the high-dose bystander verified that amongst different investigated groups, when medium exchange was applied 4 h after the irradiation, the largest bystander signaling appeared in comparison with the 1 h irradiation. Moreover, when gH2AX assay was exerted 1 h, 4 h, and 24 h-post medium sharing, the time-point of 1 h in HeLa, and also 4 h in HN5 could terminate in maximum foci with the “gH2AX enhancement ratio” of 1.27 (HeLa) and 1.72 (HN5), respectively. Additionally, the foci formation descended after the peak hitting, but it was still constantly in higher level than the control one. This general time-dependent nature of bystander induced gH2AX foci in this research was in agreement with distinct reports [18-23, 32]. Primary studies indicated the foci upward trend, which was detectable as early as 1 min, reaching the peak of 10-30 min after the irradiation [20], and supported by DSBs observation evidence in radiation-induced extracellular effects after the α particle interaction [19]. The spatiotemporal study of the bystander signaling of α particle recognized a gH2AX foci ascending trend in bystander populations, initiating as early as 2 min after the exposure, which could reach the peak at 30 min comprising two-fold increase, and after that descended but remaining still constant for 6 h in higher level than the controls [21]. DDR identical kinetic was not always illustrated in both directly-irradiated and bystander cells and it was obtained the highest level at 18 h in adjacent cells despite 30 min in target ones after the α irradiation [18]. DSBs induction time-dependency was also indicated at the peak of 1 h, 30 min [22, 23] and even 12 to 48 h after the high-LET radiation [32]. However, the considerable numbers of investigations were implemented by high-LET radiation par-

ticularly in low-dose levels, whereas data of this study were allocated to RIBE triggered by high-dose level of low-LET irradiation.

Up to now, the noticeable variation in gH2AX formation amongst distinct reports has been observed particularly in the first hour after irradiation. Different factors like cell line, microscope, camera optical characteristics, image analysis, and foci scoring strategies could play an important role in this discrepancy [33]. Considering these factors, the best time-point for gH2AX analysis was earlier indicated at about 30 min to 1 h after the exposure, when the size and intensity of the majority of induced foci could be considered as appropriate for the valid scoring [33]. Consequently, our report of high-dose bystander compatible with low-dose results also confirmed 1 h as an appropriate time for the scoring. However, 4 h incubation time of HN5 reached the maximum foci formation which might imply the difference of resistant cell lines.

In agreement with many reports findings, we observed the foci persisted even for 24 h after medium transfer, being steadily in higher level than the control. Thus, another challenging issue could be the “persistent” or “residual” gH2AX foci nature and chief cause. It has been indicated the persistent foci observation even at the time-point that complex DSB repair expected to be completed [34] and in this regard the foci long term persistence up to 7 days has been reported [32]. Additionally, the association between DSBs and gH2AX has been supported by some reports, suggesting that each DSB could be compatible with one gH2AX foci, but the reverse relationship may not exist [17]. This notion was elicited from recent investigations that larger persistent foci could be formed as a function of permanent chromatin structural changes [34], not merely reflecting unrepaired DSBs [35]. It could be concluded that the persistent foci at the time-point of 24 h in the current study might be as a result of unrepaired DSBs or chromatin structural changes.

The underpinning of RIBE might be considered as a DNA DSBs role, which was investigated by confirmatory studies [11, 12] and indicated DNA damage as a prerequisite for RIBE [13, 14]. As illustrated by early evidence, unrepaired DNA DSBs could activate the “damage-sensing process”, leading to lethality as the most deleterious effect of ionizing radiation which results in mitotic cell death or apoptosis [36]. However, DNA damage-triggered apoptosis has been contradicted, as well [27]. Concerning cell death in this research, RIBE was proposed as clonogenic survival reduction in neighboring cells receiving 1.5 Gy in comparison with cells directly-exposed by 1.5 Gy, particularly in HN5 as a radioresistant tumor cell line. Noteworthy, cell death of bystander group was more than 2 Gy direct-irradiation, presenting remarkable effect of RIBE compared to the 2 Gy irradiation. Given another cell killing alternative, proof of apoptosis induction in bystander cells has been stated based on experimental settings or cell types as well as contradictory outcomes [31]. Despite the report indicating enhanced apoptosis induction by inhomogeneous irradiation compared to uniform one at 24 h and 48 h after the irradiation [30], our results may not propose the firm agreement with them since we observed the gradual increase in apoptosis of bystander cell populations, which was not statistically significant. Elucidation of the relationship between radiation-induced apoptosis and clonogenic survival regarded complex since apoptosis could be considered as a mitotic death or/and non-mitotic death consequence [37] and there is still a big controversy surrounding the apoptosis involvement in radiation-induced cell death [27]. In this research, the mitotic death made a substantial contribution to cell killing in comparison with apoptosis and there might be some explanation for this discrepancy, including cell line and irradiation strategy. Some cell types including epithelial or mesenchymal-based tumors have not represented any association be-

tween the apoptosis incidence and clonogenic cell death, based on the late apoptosis and the post mitotic cell death [27]. Moreover, comparing with the single dose, the favorable aspect of fractionated radiotherapy has been indicated in apoptosis induction [27]. Therefore, more investigations incorporated into in-vivo studies are required to elucidate the proposed relationship clearly.

Conclusion

This in vitro investigation provided evidence supporting the bystander contribution in high-dose levels, implying that the response was not inactive. More importantly, high-dose bystander-induced gH2AX foci as a surrogate marker of DNA damage had a time-dependent mannerism. The clonogenic cell death in comparison with the apoptosis was also elicited as a consequence of bystander-induced DNA damage. However, clarifying their contribution and relationship required further confirmations.

Acknowledgment

The authors would like to express their thanks to the Radiation Therapy Department of Cancer Institute as well as Novin Medical Radiation Institute.

Authors' Contribution

F. Pakniyat conceived the idea and wrote the article. H. Mozdarani and HA. Nedaie made substantial contributions to the design of the study. A. Mahmoudzadeh, S. Gholami and M. Salimi helped F. Pakniyat in method implementation. F. Pakniyat drafted the manuscript and H. Mozdarani was responsible for the overall supervision of the work, as a corresponding author. All the authors read, modified, and approved the final version of the manuscript.

Ethical Approval

The Ethics Committee of Tehran University of Medical Sciences approved the protocol of

the study (IR.TUMS.REC.1395.2464).

Funding

This study was supported by Tehran University of Medical Sciences, Tehran, Iran [grant number 30958-30-04-94] and Tarbiat Modares University (grant number IG-39711).

Conflict of Interest

None

References

1. Nagasawa H, Little JB. Induction of sister chromatid exchanges by extremely low doses of α -particles. *Cancer Research*. 1992;**52**(22):6394-6. PubMed PMID: 1423287.
2. Morgan WF. Non-targeted and delayed effects of exposure to ionizing radiation: I. Radiation-induced genomic instability and bystander effects in vitro. *Radiation Research*. 2003;**159**(5):567-80. doi: 10.1667/0033-7587(2003)159[0567:NA DEOE]2.0.CO;2. PubMed PMID: 12710868.
3. Morgan WF. Non-targeted and delayed effects of exposure to ionizing radiation: II. Radiation-induced genomic instability and bystander effects in vivo, clastogenic factors and transgenerational effects. *Radiation Research*. 2003;**159**(5):581-96. doi: 10.1667/0033-7587(2003)159[0581:NA DEOE]2.0.CO;2. PubMed PMID: 12710869.
4. Buonanno M, De Toledo SM, Pain D, Azzam EI. Long-term consequences of radiation-induced bystander effects depend on radiation quality and dose and correlate with oxidative stress. *Radiation Research*. 2011;**175**(4):405-15. doi: 10.1667/RR2461.1. PubMed PMID: 21319986. PubMed PMCID: PMC3106980.
5. Mothersill C, Seymour CB. Bystander and delayed effects after fractionated radiation exposure. *Radiation Research*. 2002;**158**(5):626-33. doi: 10.1667/0033-7587(2002)158[0626:BADE AF]2.0.CO;2. PubMed PMID: 12385640.
6. Maguire P, Mothersill C, Seymour C, Lyng FM. Medium from irradiated cells induces dose-dependent mitochondrial changes and BCL2 responses in unirradiated human keratinocytes. *Radiation Research*. 2005;**163**(4):384-90. doi: 10.1667/rr3325. PubMed PMID: 15799693.
7. Blyth BJ, Sykes PJ. Radiation-induced bystander effects: what are they, and how relevant are they to human radiation exposures? *Radiation Research*. 2011;**176**(2):139-57. doi: 10.1667/rr2548.1. PubMed PMID: 21631286.
8. Mothersill C, Seymour C. Medium from irradiated human epithelial cells but not human fibroblasts reduces the clonogenic survival of unirradiated cells. *Int J Radiat Biol*. 1997;**71**(4):421-7. doi: 10.1080/095530097144030. PubMed PMID: 9154145.
9. Azzam EI, De Toledo SM, Little JB. Direct evidence for the participation of gap junction-mediated intercellular communication in the transmission of damage signals from α -particle irradiated to nonirradiated cells. *Proc Natl Acad Sci U S A*. 2001;**98**(2):473-8. doi: 10.1073/pnas.98.2.473. PubMed PMID: 11149936. PubMed PMCID: PMC14611.
10. Karagiannis TC, El-Osta A. DNA damage repair and transcription: Double-strand breaks: signaling pathways and repair mechanisms. *Cell Mol Life Sci*. 2004;**61**(17):2137-47. doi: 10.1007/s00018-004-4174-0. PubMed PMID: 15338043.
11. Little JB, Nagasawa H, Li GC, Chen DJ. Involvement of the nonhomologous end joining DNA repair pathway in the bystander effect for chromosomal aberrations. *Radiation Research*. 2003;**159**(2):262-7. doi: 10.1667/0033-7587(2003)159[0262:IOTNEJ]2.0.CO;2. PubMed PMID: 12537532.
12. Nagasawa H, Huo L, Little JB. Increased bystander mutagenic effect in DNA double-strand break repair-deficient mammalian cells. *Int J Radiat Biol*. 2003;**79**(1):35-41. PubMed PMID: 12556329.
13. Yang H, Asaad N, Held KD. Medium-mediated intercellular communication is involved in bystander responses of X-ray-irradiated normal human fibroblasts. *Oncogene*. 2005;**24**(12):2096-103. doi: 10.1038/sj.onc.1208439. PubMed PMID: 15688009.
14. Hill MA, Ford JR, Clapham P, Marsden SJ, Stevens DL, Townsend KM, Goodhead DT. Bound PCNA in nuclei of primary rat tracheal epithelial cells after exposure to very low doses of plutonium-238 α particles. *Radiat Res*. 2005;**163**(1):36-44. doi: 10.1667/RR3282. PubMed PMID: 15606305.
15. Kashino G, Suzuki K, Matsuda N, Kodama S, Ono K, Watanabe M, Prise KM. Radiation induced bystander signals are independent of DNA damage and DNA repair capacity of the irradiated cells. *Mutat Res*. 2007;**619**(1-2):134-8. doi: 10.1016/j.mrfmmm.2007.02.005. PubMed PMID: 17395217. PubMed PMCID: PMC3004241.
16. Prise KM, Folkard M, Kuosaitė V, Tartier L, Zyuzikov N, Shao C. What role for DNA damage and repair in the bystander response? *Mutat Res*. 2006;**597**(1-2):1-4. doi: 10.1016/j.mrfmmm.2005.06.034. PubMed PMID: 16414091.

17. Mah LJ, El-Osta A, Karagiannis TC. γ H2AX: a sensitive molecular marker of DNA damage and repair. *Leukemia*. 2010;**24**(4):679-86. doi: 10.1038/leu.2010.6. PubMed PMID: 20130602.
18. Sokolov MV, Smilenov LB, Hall EJ, Panyutin IG, Bonner WM, Sedelnikova OA. Ionizing radiation induces DNA double-strand breaks in bystander primary human fibroblasts. *Oncogene*. 2005;**24**(49):7257-65. doi: 10.1038/sj.onc.1208886. PubMed PMID: 16170376.
19. Hu B, Han W, Wu L, Feng H, Liu X, Zhang L, et al. In situ visualization of DSBs to assess the extranuclear/extracellular effects induced by low-dose α -particle irradiation. *Radiation Research*. 2005;**164**(3):286-91. doi: 10.1667/RR3415.1.
20. Rogakou EP, Boon C, Redon C, Bonner WM. Megabase chromatin domains involved in DNA double-strand breaks in vivo. *J Cell Biol*. 1999;**146**(5):905-16. doi: 10.1083/jcb.146.5.905. PubMed PMID: 10477747. PubMed PMCID: PMC2169482.
21. Hu B, Wu L, Han W, Zhang L, Chen S, Xu A, et al. The time and spatial effects of bystander response in mammalian cells induced by low dose radiation. *Carcinogenesis*. 2006;**27**(2):245-51. doi: 10.1093/carcin/bgi224. PubMed PMID: 16150894.
22. Yang H, Anzenberg V, Held KD. The time dependence of bystander responses induced by iron ion radiation in normal human skin fibroblasts. *Radiat Res*. 2007;**168**(3):292-8. doi: 10.1667/RR0864.1. PubMed PMID: 17705636.
23. Han W, Wu L, Hu B, Zhang L, Chen S, Bao L, et al. The early and initiation processes of radiation-induced bystander effects involved in the induction of DNA double strand breaks in non-irradiated cultures. *Br J Radiol*. 2007;**80**(Spec No 1):S7-12. doi: 10.1259/bjr/44550200. PubMed PMID: 17704329.
24. Desouky O, Ding N, Zhou G. Targeted and non-targeted effects of ionizing radiation. *Journal of Radiation Research and Applied Sciences*. 2015;**8**(2):247-54. doi: 10.1016/j.jrras.2015.03.003.
25. Turesson I, Carlsson J, Brahme A, Glimelius B, Zackrisson B, et al. Biological response to radiation therapy. *Acta Oncol*. 2003;**42**(2):92-106. doi: 10.1080/02841860310004959. PubMed PMID: 12801128.
26. Prasanna A, Ahmed MM, Mohiuddin M, Coleman CN. Exploiting sensitization windows of opportunity in hyper and hypo-fractionated radiation therapy. *J Thorac Dis*. 2014;**6**(4):287. doi: 10.3978/j.issn.2072-1439.2014.01.14. PubMed PMID: 24688774. PubMed PMCID: PMC3968552.
27. Balcer-Kubiczek EK. Apoptosis in radiation therapy: a double-edged sword. *Exp Oncol*. 2012;**34**(3):277-85. PubMed PMID: 23070013.
28. Billena C, Khan AJ. A Current Review of Spatial Fractionation: Back to the Future? *Int J Radiat Oncol Biol Phys*. 2019;**104**(1):177-87. doi: 10.1016/j.ijrobp.2019.01.073. PubMed PMID: 30684666. PubMed PMCID: PMC7443362.
29. Gholami S, Nedaie HA, Longo F, Ay MR, Dini SA, Meigooni AS. Grid Block Design Based on Monte Carlo Simulated Dosimetry, the Linear Quadratic and Hug-Kellerer Radiobiological Models. *J Med Phys*. 2017;**42**(4):213-21. doi: 10.4103/jmp.JMP_38_17. PubMed PMID: 29296035. PubMed PMCID: PMC5744449.
30. Zhang D, Zhou T, He F, Rong Y, Lee SH, Wu S, Zuo L. Reactive oxygen species formation and bystander effects in gradient irradiation on human breast cancer cells. *Oncotarget*. 2016;**7**(27):41622-36. doi: 10.18632/oncotarget.9517. PubMed PMID: 27223435. PubMed PMCID: PMC5173083.
31. Mah LJ, El-Osta A, Karagiannis TC. GammaH2AX as a molecular marker of aging and disease. *Epigenetics*. 2010;**5**(2):129-36. doi: 10.4161/epi.5.2.11080. PubMed PMID: 20150765.
32. Sedelnikova OA, Nakamura A, Kovalchuk O, Kolturbash I, Mitchell SA, Marino SA, Brenner DJ, Bonner WM. DNA double-strand breaks form in bystander cells after microbeam irradiation of three-dimensional human tissue models. *Cancer Res*. 2007;**67**(9):4295-302. doi: 10.1158/0008-5472.CAN-06-4442. PubMed PMID: 17483342.
33. Rothkamm K, Horn S. gamma-H2AX as protein biomarker for radiation exposure. *Ann Ist Super Sanita*. 2009;**45**(3):265-71. PubMed PMID: 19861731.
34. Costes SV, Chiolo I, Pluth JM, Barcellos-Hoff MH, Jakob B. Spatiotemporal characterization of ionizing radiation induced DNA damage foci and their relation to chromatin organization. *Mutat Res*. 2010;**704**(1-3):78-87. doi: 10.1016/j.mrrev.2009.12.006. PubMed PMID: 20060491. PubMed PMCID: PMC3951968.
35. Rothkamm K, Barnard S, Moquet J, Ellender M, Rana Z, Burdak-Rothkamm S. DNA damage foci: Meaning and significance. *Environmental and Molecular Mutagenesis*. 2015;**56**(6):491-504. doi: 10.1002/em.21944. PubMed PMID: 25773265.
36. Salimi M, Mozdarani H. [gamma]-H2AX as a protein biomarker for radiation exposure response

in ductal carcinoma breast tumors: Experimental evidence and literature review. *International Journal of Radiation Research*. 2014;**12**(1):1.
37. Prise KM, Schettino G, Folkard M, Held KD. New

insights on cell death from radiation exposure. *Lancet Oncol*. 2005;**6**(7):520-8. doi: 10.1016/S1470-2045(05)70246-1. PubMed PMID: 15992701.